Inverse axial mounting stiffness design for lithographic projection lenses

Yuan Wen-quan,* Shang Hong-bo, and Zhang Wei

State Key Laboratory of Applied Optics, Changchun Institute of Optics, Fine Mechanics and Physics, The Chinese Academy of Sciences, Changchun 130033, China

*Corresponding author: yuanwq@sklao.ac.cn

Received 26 May 2014; revised 28 July 2014; accepted 28 July 2014; posted 29 July 2014 (Doc. ID 212819); published 27 August 2014

In order to balance axial mounting stiffness of lithographic projection lenses and the image quality under dynamic working conditions, an easy inverse axial mounting stiffness design method is developed in this article. Imaging quality deterioration at the wafer under different axial vibration levels is analyzed. The desired image quality can be determined according to practical requirements, and axial vibrational tolerance of each lens is solved with the damped least-squares method. Based on adaptive interval adjustment, a binary search algorithm, and the finite element method, the axial mounting stiffness of each lens can be traveled in a large interval, and converges to a moderate numerical solution which makes the axial vibrational amplitude of the lens converge to its axial vibrational tolerance. Model simulation is carried out to validate the effectiveness of the method. © 2014 Optical Society of America

OCIS codes: (110.5220) Photolithography; (110.3000) Image quality assessment; (220.1010) Aberrations (global); (220.1140) Alignment; (220.3740) Lithography; (220.4880) Optomechanics.

http://dx.doi.org/10.1364/AO.53.005720

1. Introduction

All the lithographic projection lenses suffer imaging quality deterioration caused by aberrations [1–3], which is a bottleneck to improving lithographic resolution. Reasons for their aberrations may come from tolerances of mechanical references, operational levels of shock, vibration, pressure, and temperature variations [4]. To reduce such negative effects on aberrations of these high-performance lenses, they are usually mounted in symmetrically flexural or kinematic manners [5–12], for deformation on their surface due to tolerances of mounting datum will be minimized and their alignments can be retained during exposure to survival levels of these environments. Actually there are many merits for mounting lenses in these kinds of compliant means, but the mounting stiffness needs to be carefully designed in application. This is because if the stiffness is high, tolerances of the mechanical references need to be stringent, which will be costly in manufacturing [13–16]. Low mounting stiffness will relax mechanical tolerances, but every lens in a lithographic objective vibrates relatively easily due to the dynamic environment, and the focal plane of the optical system vibrates too. This effect is comparable to shaking a camera when taking a photograph, resulting in a blurred image. Therefore, there needs to be an equilibrium point between manufacturing costs and focus stability in mounting stiffness design for lithographic projection lenses. And a good equilibrium point, in other words, an apropos mounting stiffness design, can make the lithographic projective meet the desired requirements of focus stability at least costs.

Unlike other inverse problems, using requirements of focus stability to infer mounting stiffness of compliant manners in an objective is difficult, for there is not a unique group of displacements solutions of lenses under random vibration. In addition, the gravity centers of objectives are usually not at their horizontal mounting datum; therefore, the

1559-128X/14/255720-06$15.00/0

whole bodies oscillate coupled with horizontal vibration when they work. Since mounting stiffness in horizon and roll or pitch cannot be uncoupled according to random vibrational motions of the lenses, full inverse mounting stiffness design becomes impossible. However, beeline defined by the gravity center of the projection objective and the geometrical center of its mounting points is nearly perpendicular to the mounting datum. Vibration of lenses in the axial direction can therefore be considered uncoupled from other degrees of freedom. And axial mounting stiffness of lenses can be inferred if their axial vibrational tolerances are known.

In this paper, a simple, easy programming, and effective inverse axial mounting stiffness design method for lenses in lithographic objective is developed. Considering the desired image quality, axial vibrational tolerances of lenses are solved with the damped least-squares method [17,18]. Consequently, several large intervals are assigned for axial mounting stiffness of lenses, and axial random vibrational displacements of lenses related to midpoints of their stiffness intervals can be analyzed with the finite element (FE) method. Comparing the FE results with related tolerances, the stiffness intervals are changed with a binary search algorithm [19,20] and adaptive interval adjustment [21,22]. The above process is repeated until differences between the FE results and related tolerances are less than a predefined small positive value; the related axial stiffness then is the numerical solution.

This article is constructed as follows. The inverse axial mounting stiffness design problem is described with a lithographic projection optical system in Section 2. The main procedure to solve the problem and its key technology are demonstrated in Section 3. Results of the problem are presented in Section 4. Conclusions are summarized in Section 5.

2. Problematic Description

Not only are lenses compliantly mounted in the projection objective, but also projection objectives are compliantly mounted in lithographic tools too, for vibrations from lithographic tools can infect the whole objective slightly. A typical projection objective structure and several kinds of compliant structures for mounting lenses are depicted in Fig. 1.

The projection optical system studied in this article is from a Japanese patent in 2005 [23]. The optical system consists of 20 lenses, and its working wavelength is 193 nm. Random vibrational excitation on the mechanical interface of the lithographic objective can be measured with accelerometers, and the acceleration power spectral density (APSD) can be obtained via spectral analysis. Based on multiple vibrational measuring of a 193 nm lithographic tool, a typical axial APSD specification on the mechanical interface of the projection objective under work can be presented. The projection optical system and the axial APSD specification are depicted in Fig. 2.

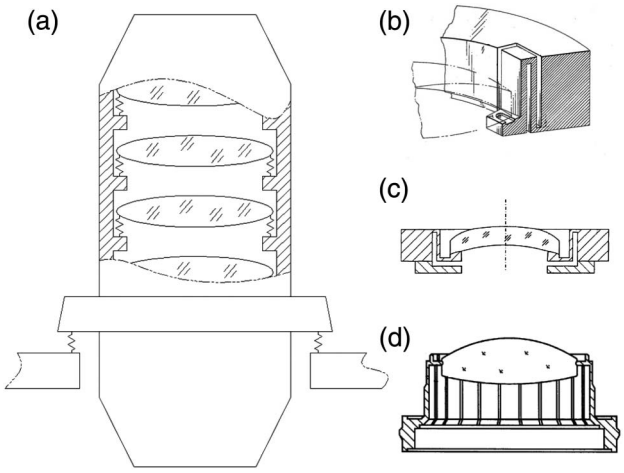

Fig. 1. Schematic of compliant mounting manners. (a) Compliant manners of objective and lenses. (b) Compliant means from [7]. (c) Compliant means from [11]. (d) Compliant means from [12].

Unless lenses are rigidly mounted in the projection objective, they will obviously vibrate relatively when lithographic tools work. As an inevitable result, the focal plane of the optical system vibrates too and the image at the wafer will blur. In axial direction, the problem can be described as: how to design axial mounting stiffness of every lens for balancing manufacturing costs and optical performance under dynamic working conditions.

3. Solution

A. Main Procedure of Inverse Axial Stiffness Design

To minimize axial mounting stiffness of the lenses with constraint of image quality, the inverse axial mounting stiffness design can also be considered as an optimization problem here. And it can be stated as

$$\text{Minimize}\, K_n (n = 1, 2, 3 \ldots 20), \tag{1}$$

$$\text{Subject to}\, \Delta F \le \Delta F^{\text{desired}}, \tag{2}$$

where K_n is the axial mounting stiffness of lens member n; ΔF is image quality at the wafer of projection objective under dynamic working conditions; $\Delta F^{\text{desired}}$ defines the desired image quality. Since

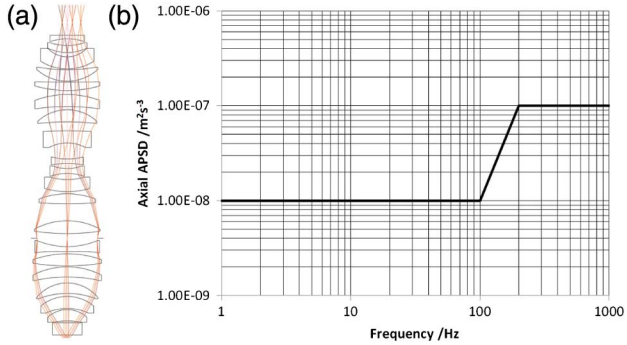

Fig. 2. Model illustration. (a) Projection optical system [23]. (b) Axial APSD specification.

there are no direct relations between mechanical parameters K_n and optical parameter $\Delta F^{\text{desired}}$, $\Delta F^{\text{desired}}$ needs to be expressed as axial vibration tolerance $\Delta X_n^{\text{desired}}$ of each lens with optical analysis. On the other hand, axial random vibrational displacement ΔX_n of each lens can be analyzed with FE software if K_n is assigned. Now, changing values of K_n and comparing ΔX_n with $\Delta X_n^{\text{desired}}$ can determine whether K_n is suitable. And if all ΔX_n converge to the related $\Delta X_n^{\text{desired}}$, related K_n is the numerical solution and inverse axial stiffness design finishes.

Unlike other inverse problems, there are 20 axial mounting stiffness variables $K_n(n = 1, 2, 3, \ldots 20)$ in all here, and variation of each one will change random vibrational responses of the other lenses. Traditionally, an evolutionary algorithm [24–27] can be applied to solve such problems. But a simple method, which is much easier in programing, is developed here. Its major steps are described as follows: First, 20 groups of large intervals $(K_{bn}^i, K_{en}^i)(i = 1; n = 1, 2, 3, \ldots 20)$ for the axial mounting stiffness of lenses are assigned, and $K_n^i = (K_{bn}^i + K_{en}^i)/2$ is set as the initial axial mounting stiffness. Here, K_b denotes the beginning of the interval, K_e denotes the ending, i is the iteration step, and $i = 1$ denotes initial status. A large initial interval $(0, 10^{12}$ N/m) is set for each interval in this article. Then, axial random vibrational displacement ΔX_n^i of each lens can be analyzed with FE software. Third, compare ΔX_n^i with $\Delta X_n^{\text{desired}}$ (obtained in axial vibrational tolerance analysis), and reassign the intervals (K_{bn}^i, K_{en}^i) with a binary search algorithm, or enlarge the interval via adaptive interval adjustment when K_n^i converges while ΔX_n^i do not converge to $\Delta X_n^{\text{desired}}$, and do the next loop of FE analysis. When each ΔX_n^i converges to $\Delta X_n^{\text{desired}}$, the related K_n^i can be obtained and the inverse axial stiffness design is finished.

The main procedure of the inverse axial stiffness design is depicted in Fig. 3. $\varepsilon_{\Delta x}$ is the tolerance of ΔX_n^i, ε_K is the tolerance factor of K_n^i, and f is a scale factor. The portion in blue in Fig. 3 describes the solution of $\Delta X_n^{\text{desired}}$, and its details are described in Subsection 3.B. The portions in orange and green are iterative solution procedures of "axial mounting stiffness–random vibration analysis." The portion in green, which is in the red dashed box, describes applications of the binary search algorithm and adaptive interval adjustment in detail, and they can be realized with several "if…then…" constructions easily. Random vibration analysis of the model with FE software is described in Subsection 3.C.

B. Axial Vibrational Tolerances Analysis

When lithographic tools works, the desired imaging quality under environmental axial vibration can be depicted as

$$A\Delta X^{\text{desired}} = \Delta F^{\text{desired}}, \tag{3}$$

where $\Delta X^{\text{desired}}$ is the vector form of $\Delta X_n^{\text{desired}}$, A is a $m \times 40$ sensitive matrix, which can be obtained by

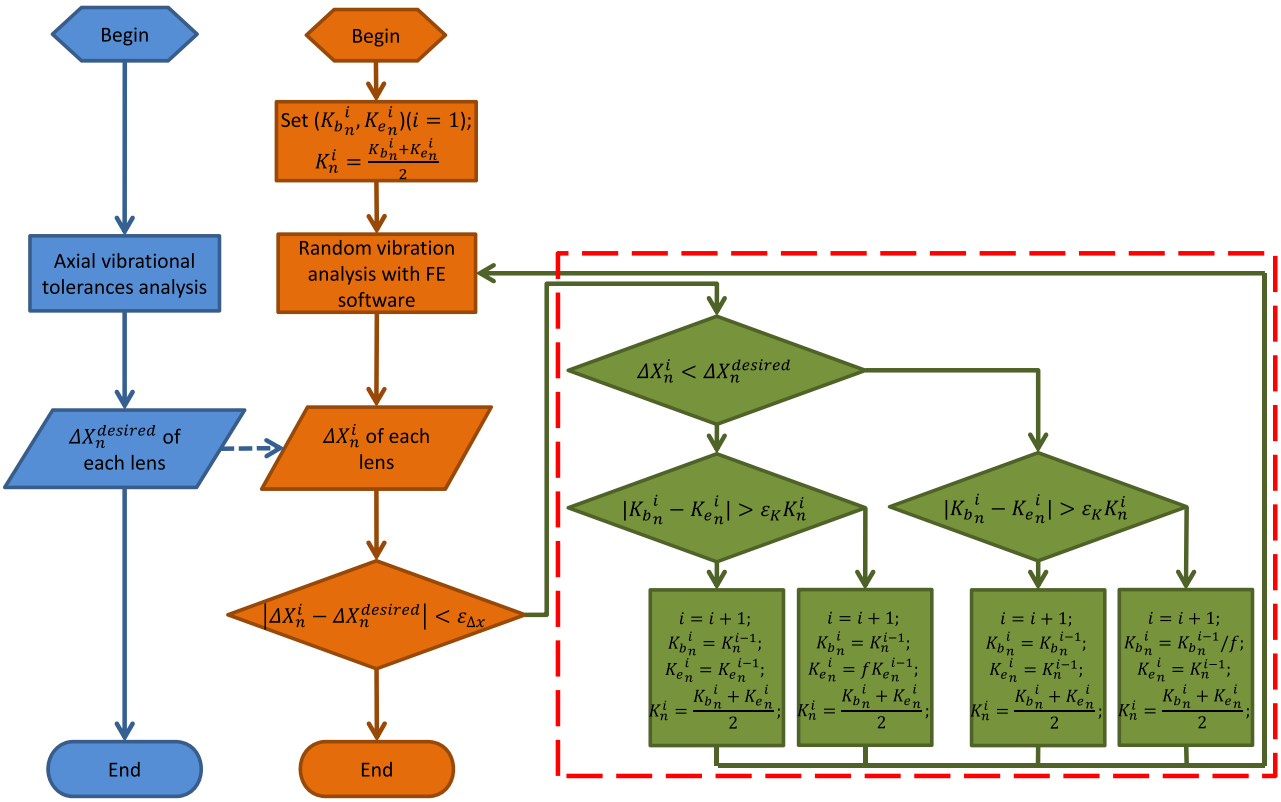

Fig. 3. Flow chart of inverse axial stiffness design procedure.

optical system design data. Since the value of m is usually much greater than 40, $\Delta X^{\text{desired}}$ needs to be obtained by the damped least-squares method if $\Delta F^{\text{desired}}$ is known. First, an aberration estimating function $\Psi(\Delta X^{\text{desired}})$ can be easily established as

$$\Psi(\Delta X^{\text{desired}}) = (A\Delta X^{\text{desired}} - \Delta F^{\text{desired}}) + p^2 \Delta X^{\text{desired}T} \Delta X^{\text{desired}}, \quad (4)$$

where p is the damped factor. Then, if the optical system under the vibration environment meets the design requirements, there must be

$$\text{Min}\{\Psi(\Delta X^{\text{desired}})\}. \quad (5)$$

Or Eq. (5) can be transformed to

$$(A^T A + p^2 I)\Delta X^{\text{desired}} = A^T \Delta F^{\text{desired}}, \quad (6)$$

where I is the identity matrix. And the solution of Eq. (6) is

$$\Delta X^{\text{desired}} = (A^T A + p^2 I)^{-1} A^T \Delta F^{\text{desired}}. \quad (7)$$

For convenient calculation, Eq. (7) can be transformed to Eq. (8) via singular value decomposition [28]:

$$\Delta X^{\text{desired}} = V\left\{\left(\Sigma^T \Sigma + p^2 I\right)^{-1} \Sigma^T\right\} U^T \Delta F^{\text{desired}}, \quad (8)$$

where $A = U\Sigma V^T$. Therefore, if imaging quality deterioration $\Delta F^{\text{desired}}$ induced by axial environmental vibration is assigned, axial vibration tolerance $\Delta X^{\text{desired}}$ of lenses can be easily calculated with Eq. (8).

C. Random Vibration Analysis

Axial random vibrational displacements of the projection objective under work are analyzed with the FE software ANSYS Academic Research 15.0 in this article. And in establishment of its FE model, mechanical parts of the projection objective are simplified as rigid beam and mass elements. Lenses are simplified as mass elements too. Connections between lenses and mechanical parts are simplified as springs which are compliant in the axial direction while fully constrained in other degrees of freedom. When the whole model is established, its constrained frequencies and mode shapes under work can be analyzed. Then, axial APSD excitations [1–1000 Hz, shown in Fig. 2(b)] from lithographic tools are applied on the mechanical interface of the projection objective, and the relative displacement power spectral density of each lens at the axial direction can be solved with the mode combination method. Integrating the spectrums, 3σ axial displacement solution of each lens under work can be obtained.

To depict positions and aspects of the lenses clearly, they are drawn with area elements in ANSYS Academic Research 15.0. The whole FE model and one of its random vibrational results are shown in Fig. 4, and units in Fig. 4 are SI.

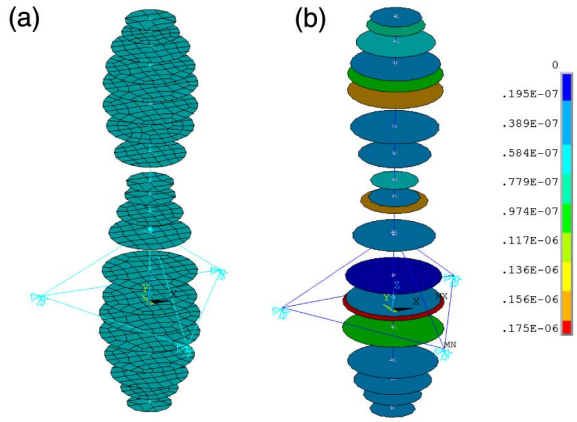

Fig. 4. Random vibration analysis of the projection objective with ANSYS Academic Research 15.0. (a) FE model of the projection objective. (b) One 3σ displacements solution of random vibration analysis.

4. Results

In order to determine $\Delta F^{\text{desired}}$ of the projection optical system, a typical 90 nm projected image of the mask is set as Fig. 5(a). The illumination is a dipole illumination, which is shown in Fig. 5(b). The image qualities at different wafer positions, which

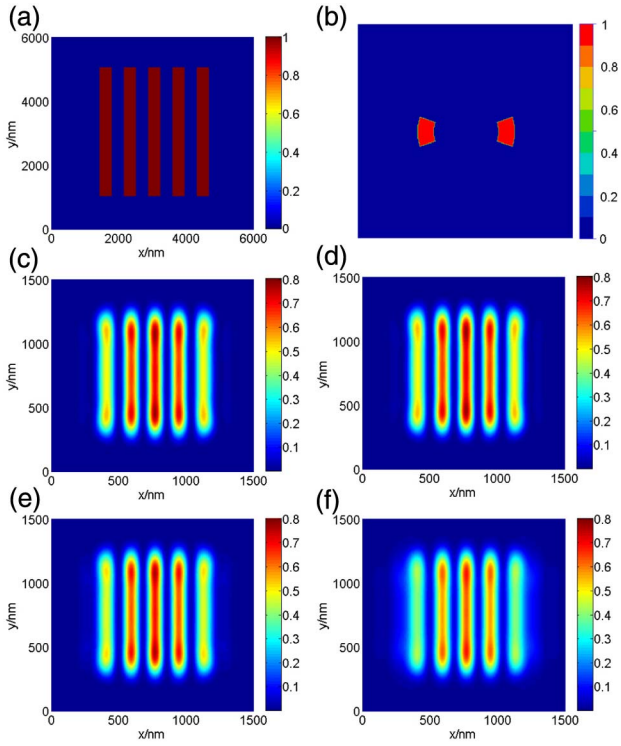

Fig. 5. Evaluation of image quality. (a) Mask. (b) Dipole. (c) Image quality at best focal plane. (d) Image at ±30 nm axially offset from the best focal plane. (e) Image at ±100 nm axially offset from the best focal plane. (f) Image at ±200 nm axially offset from the best focal plane.

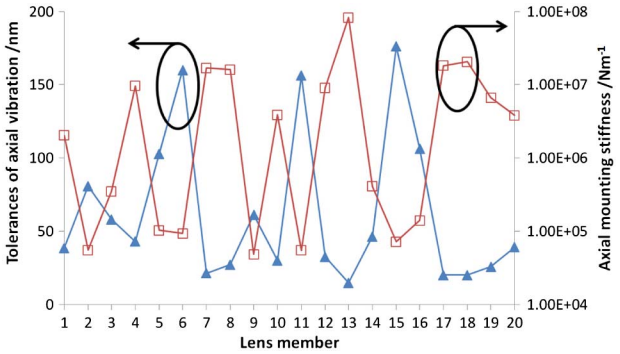

Fig. 6. Design results of the axial tolerances for lenses and their related axial mounting stiffness.

are axially offset from the best focal plane, are analyzed with CODE V software. Several typical image results, which are depicted in form of relative intensity, are shown in Figs. 5(c)–5(f). In addition, Rayleigh depth of focus criterion [29] has stated that

$$\mathrm{DOF} = k_2 \frac{\lambda}{\mathrm{NA}^2}, \tag{9}$$

where DOF is depth of focus, k_2 is process-dependent constant, λ is working wavelength, NA is numerical aperture. If k_2, λ, and NA are set as 1, 193 nm, and 0.75, then DOF can be obtained as less than 343 nm. That is to say, the axial focal stability of the optical system needs to be less than ± 172 nm at maximum.

Considering vibration of other degrees of freedom may also induce image blur, the desired focal stability in the axial direction is determined as less than ± 30 nm here. Axial vibration tolerances $\Delta X_n^{\mathrm{desired}}$ of each lens can now be calculated with the method in Subsection 3.B, and the axial mounting stiffness of each lens can also be obtained easily. Both of the results are shown in Fig. 6.

5. Conclusion

To balance axial mounting stiffness of lenses in the lithographic objective and the image quality under dynamic working condition, an easy inverse axial mounting stiffness design method is developed in this article. In this method, axial vibrational tolerance of each lens in the optical system is solved with damped least-squares according to the desired image quality. Several large intervals are initially assigned for axial mounting stiffness of lenses, and axial random vibrational displacement of each lens related to midpoints of its stiffness interval is analyzed with the FE method. Comparing the FE results with related tolerances, the stiffness interval of each lens can be reassigned with a binary search algorithm and adaptive interval adjustment from the comparison. Repeating the above process until the FE results converge to related tolerances, the related axial stiffness is then the solution. Model simulation in this article validates the effectiveness of the method.

This work is supported by the National 02 Project of China (grant 2009ZX02205).

References

1. T. Brunner, "Impact of lens aberrations on optical lithography," IBM J. Res. Dev. **41**, 57–67 (1997).
2. K. Matsumoto, T. Matsuyama, and S. Hirukawa, "Analysis of imaging performance degradation," Proc. SPIE **5040**, 131–138 (2003).
3. P. Graeupner, R. B. Garreis, A. Goehnermeier, T. Heil, M. Lowisch, and D. G. Flagello, "Impact of wavefront errors on low k1 processes at extremely high NA," Proc. SPIE **5040**, 119–130 (2003).
4. P. R. Yoder, *Opto-Mechanical Systems Design*, 3rd ed. (CRC Press, 2006).
5. B. Saggin, M. Tarabini, and D. Scaccabarozzi, "Infrared optical element mounting techniques for wide temperature ranges," Appl. Opt. **49**, 542–548 (2010).
6. J. J. Bacich, "Precision lens mounting," U.S. patent 4,733,945 (29 March 1988).
7. A. Ahmad and R. L. Huse, "Mounting for high resolution projection lenses," U.S. patent 4,929,054 (29 May 1990).
8. H. Holderer, P. Rummer, and M. Trunz, "Assembly of optical element and mount," U.S. patent 6,229,657 (8 May 2001).
9. D. C. Watson and W. T. Novak, "Kinematic lens mounting with distributed support and radial flexure," U.S. patent 6,239,924 (29 May 2001).
10. E. Merz and J. Becker, "Optical system, in particular projection-illumination unit used in microlithography," U.S. patent 6,307,688 (23 October 2001).
11. T. Schletterer, "Elastic lens holder," U.S. patent 6,560,045 (6 May 2003).
12. K. Beck, B. Gellrich, H. Holderer, T. Petasch, C. Roesch, and A. Kohl, "Adjustment arrangement of an optical element," U.S. patent 7,193,794 (20 March 2007).
13. C. C. Wu, Z. Chen, and G. R. Tang, "Component tolerance design for minimum quality loss and manufacturing cost," Comput. Ind. **35**, 223–232 (1998).
14. S. Jin, C. Zheng, K. Yu, and X. Lai, "Tolerance design optimization on cost–quality trade-off using the Shapley value method," J. Manuf. Syst. **29**, 142–150 (2010).
15. R. Curran, A. Kundu, S. Raghunathan, D. Eakin, and R. McFadden, "Influence of manufacturing tolerance on aircraft direct operating cost (DOC)," J. Mater. Process. Technol. **138**, 208–213 (2003).
16. L. Andolfatto, F. Thiébaut, C. Lartigue, and M. Douilly, "Quality- and cost-driven assembly technique selection and geometrical tolerance allocation for mechanical structure assembly," J. Manuf. Syst. **33**, 103–115 (2014).
17. J. Meiron, "Damped least-squares method for automatic lens design," J. Opt. Soc. Am. **55**, 1105–1109 (1965).
18. M. J. Kidger, "Use of the Levenberg–Marquardt (damped least squares) optimization method in lens design," Opt. Eng. **32**, 1731–1739 (1993).
19. B. B. Chhetri, S. Yang, and T. Shimomura, "Stochastic approach in the efficient design of the direct-binary-search algorithm for hologram synthesis," Appl. Opt. **39**, 5956–5964 (2000).
20. B. Shen, P. Wang, and R. Menon, "Optimization and analysis of 3D nanostructures for power-density enhancement in ultrathin photovoltaics under oblique illumination," Opt. Express **22**, A311–A319 (2014).
21. A. Winman, P. Hansson, and P. Juslin, "Subjective probability intervals: How to reduce overconfidence by interval evaluation," J. Exp. Psychol. Learn. Mem. Cogn. **30**, 1167–1175 (2004).
22. H. Hayakawa and T. Shibata, "Block-matching-based motion field generation utilizing directional edge displacement," Comput. Elect. Eng. **36**, 617–625 (2010).
23. Y. Omura, "Projection exposure methods and apparatus, and projection optical systems," U.S. patent 6,864,961 (8 March 2005).

24. M. Currie and C. Olson, "Improved optical pulse propagation in water using an evolutionary algorithm," Opt. Express **19**, 10923–10930 (2011).
25. N. Yamada and T. Ijiro, "Design of wavelength selective concentrator for micro PV/TPV systems using evolutionary algorithm," Opt. Express **19**, 13140–13149 (2011).
26. C. C. Olson, R. T. Schermer, and F. Bucholtz, "Tailored optical force fields using evolutionary algorithms," Opt. Express **19**, 18543–18557 (2011).
27. M. Donelli, "Design of broadband metal nanosphere antenna arrays with a hybrid evolutionary algorithm," Opt. Lett. **38**, 401–403 (2013).
28. X. Zhu, J. Shen, W. Liu, X. Sun, and Y. Wang, "Nonnegative least-squares truncated singular value decomposition to particle size distribution inversion from dynamic light scattering data," Appl. Opt. **49**, 6591–6596 (2010).
29. C. Mack, *Fundamental Principles of Optical Lithography: The Science of Microfabrication* (Wiley, 2007).